who is at risk? J Autism Dev Disord, 32 ; 217-224, 2002

2) Croen, L.A., Najjar, D.V., Fireman, B., et al. : Maternal and paternal age and risk of autism spectrum disorders. Arch Pediatr Adolesc Med, 161 ; 334-40, 2007

3) Croen, L.A., Yoshida, C.K., Odouli, R., et al. : Neonatal hyperbilirubinemia and risk of autism spectrum disorders. Pediatrics, 115 ; e135-138, 2005

4) Deykin, E.Y., MacMahon, B. : Pregnancy, delivery, and neonatal complications among autistic children. Am J Dis Child, 134 ; 860-864, 1980

5) Eaton, W.W., Mortensen, P.B., Thomsen, P.H., et al. : Obstetric complications and risk for severe psychopathology in childhood. J Autism Dev Disord, 31 ; 279-285, 2001

6) Finegan, J.A., Quarrington, B. : Pre-, peri-, and neonatal factors and infantile autism. J Child Psychol Psychiatry, 20 ; 119-128, 1979

7) Gillberg, C., Gillberg, I.C. : Infantile autism : a total population study of reduced optimality in the pre-, peri-, and neonatal period. J Autism Dev Disord, 13 ; 153-166, 1983

8) Glasson, E.J., Bower, C., Petterson, B., et al. : Perinatal factors and the development of autism : a population study. Arch Gen Psychiatry, 61 ; 618-627, 2004

9) Hultman, C.M., Sparén, P., Cnattingius, S. : Perinatal risk factors for infantile autism. Epidemiology, 13 ; 417-423, 2002

10) Hurst, L.D., Ellegren, H. : Sex biases in the mutation rate. Trends Genet, 14 ; 446-452, 1998

11) Juul-Dam, N., Townsend, J., Courchesne, E. : Prenatal, perinatal, and neonatal factors in autism, pervasive developmental disorder - not otherwise specified, and the general population. Pediatrics, 107 ; e63, 2001

12) Kolevzon, A., Gross, R., Reichenberg, A. : Prenatal and Perinatal Factors for Autism. Arch Pediatr Adolesc Med, 1616 ; 326-333, 2007

13) Larsson, H.J., Eaton, W.W., Madsen, K.M., et al. : Risk factors for autism : perinatal factors, parental psychiatric history, and socioeconomic status. Am J Epidemiol, 15 ; 161 ; 916-925, 2005

14) Lauritsen, M.B., Pedersen, C.B., Mortensen, P. B. : Effects of familial risk factors and place of birth on the risk of autism : a nationwide resister-based study. J Child Psychol Psychiatry, 46 ; 963-971, 2005

15) Maimburg, R.D., Vaeth, M. : Perinatal risk factors and infantile autism. Acta Psychiatr Scand, 114 ; 257-264, 2006

16) Maimburg, R.D., Vaeth, M., Schendel, D.E., et al. : Neonatal jaundice : a risk factor for infantile autism ? Paediatr Perinat Epidemiol, 22 ; 562-568, 2008

17) Pardo, C.A., Eberhart, C.G. : The neurobiology of autism. Brain Pathol, 17 ; 434-47, 2007

18) Reichenberg, A., Gross, R., Weiser, M., et al. : Advancing paternal age and autism. Arch Gen Psychiatry, 63 ; 1026-1032, 2006

19) Schendel, D., Bhasin, T.K. : Birth weight and gestational age characteristics of children with autism, including a comparison with other developmental disabilities. Pediatrics, 121 ; 1155-1164, 2008

20) Sugie, Y., Sugie, H., Fukuda, T., et al. : Neonatal factors in infants with Autistic Disorder and typically developing infants. Autism, 9 ; 487-494, 2005

21) Williams, K., Helmer, M., Duncan, G.W., et al. : Perinatal and maternal risk factors for autism spectrum disorders in New South Wales, Australia. Child Care Health Dev, 34 ; 249-256, 2008

特集 小児科医に役立つ臨床遺伝学

Ⅳ．臨床遺伝学のトピックス

精神遅滞・てんかんの臨床遺伝学

後藤雄一　国立精神・神経センター神経研究所疾病研究第二部

Key Words
精神遅滞
脆弱X症候群
MECP2
ARX

要旨

精神遅滞をきたす代表的なX染色体上の原因遺伝子である*FMR1*，*MECP2*，*ARX*に関する研究の進歩を概観し，精神遅滞やてんかん，さらには自閉症などの症状が単一の遺伝子変異に由来する一連の疾患スペクトラムから生じる表現型であること，またその機能解析が，病態の理解と新たな治療法の開発へと繋がることを示す．

はじめに

ヒトゲノム解析研究の進歩で，新たな疾患原因遺伝子の同定が急速に進んできている．精神遅滞やてんかんにかかわる疾患についても例外でないが，そもそも精神遅滞やてんかんをきたす疾患の臨床型も原因も多彩であることから，遺伝子ですべてを明らかにすることは困難であることをまずは理解することが必要である．原因遺伝子の同定で，これまで違う疾患と考えられてきたものが単一の遺伝子変異でおきることが判明するなど，疾患を原因で分類するのか，表現型で分類するのかで疾患分類が異なってくる事態もでてきている．

原因遺伝子が同定されることには二つの利点があり，一つは遺伝子診断が可能になることである．とはいうものの，遺伝子診断が一般化するには，診断の確実性，特異性，侵襲性，経済性などとともに，診断する施設やシステムが整備されていることが重要である．わが国はこの点に大きな問題があり，早急な社会整備が必要である．

二つめは，原因遺伝子の解明から疾患の理解が進むことである．後述するように，精神遅滞をきたす原因遺伝子の一群がシナプス棘に局在する蛋白質をコードしていることが判明すると，シナプス機能不全が精神遅滞の本態ではないかという仮説がでてくることになる．また，遺伝子改変動物を作製して詳細に病態を解析し，新しい治療法を試すことができる．将来的な疾患予防や治療がみえてくるかもしれない．いずれにしても，遺伝学的手法を用いた検査や研究は診断，治療の両面で重要な役割を担っている．

本稿では，精神遅滞をきたす代表的なX染色体上の原因遺伝子である*FMR1*，*MECP2*，*ARX*に関する研究の進歩を概観し，精神遅滞やてん

0386-9806/09/¥100/頁/JCLS

かん，さらには自閉症などの症状が，単一の遺伝子変異に由来する一連の疾患スペクトラムから生じる表現型であること，またその原因は多数の遺伝子変異によるものであることが明らかになってきたことを示す．

*FMR1*に関する知見

*FMR1*遺伝子は非症候群性の精神遅滞患者で最初に同定された原因遺伝子である[1]．*FMR1*遺伝子の5'の非翻訳領域に存在するCGGリピート（正常では6～54回）が200回以上（full-mutation）に延長し，*FMR1*のプロモーター領域のCpGアイランドのメチル化が高度化してその転写が抑制されることで，mRNAやfragile X mental retardation protein（以下，FMRPと略す）が減少し，脆弱X症候群が生じることが知られている．これは機能喪失型変異である．

一方で，リピート数が60～200回のpremutationでは，脆弱X症候群関連振戦失調症候群（fragile X-associated tremor/ataxia syndrome：FXTAS）がおきることが知られており，成人では振戦や失調で発症し，下肢のニューロパチー，自律神経障害，認知機能の低下や種々の精神症状をきたすことがある[2]．この場合はFMR1 mRNAの発現が亢進している証拠が得られており，機能獲得型変異である．*FMR1*遺伝子がX染色体上にあるにもかかわらず，この二つの病態はともに男性だけではなく，X染色体不活化により女性にも症状を認めることがあるが，その頻度は低く，また症状の軽いことが知られている．

*FMR1*遺伝子をノックアウトされたマウスやハエで，病態に関する多くの知見が得られてきている．FMRPはRNA結合蛋白であり，その機能は細胞内の遺伝子発現調節，とくに翻訳の調節にかかわること，また神経細胞樹状突起の神経棘にあるシナプスの可塑性にかかわることが知られている．とくに，脆弱X症候群モデルマウス脳では，シナプスに局在する代謝型グルタミン酸受容体から入るシグナル伝達系に異常をきたしており，これが海馬での記憶機能低下の原因となっていると推測され，代謝型グルタミン酸受容体抑制薬の治療への応用が考えられている[3]．また，FMRPは前頭葉のドーパミン作動性ニューロンにもかかわっており[4]，脆弱X症候群患者で認められる精神遅滞や自閉症などの症状を説明する根拠の一つである可能性があるが，その全貌はいまだ明らかではない．

*MECP2*に関する知見

MECP2も，FMPRと同様にモデルマウスの研究でその病態が徐々に明らかにされつつある．MECP2はDNA結合蛋白であり，メチル化されたCpGに結合して他の蛋白と協働して転写を抑制するので，*MECP2*遺伝子に変異がある場合はその抑制機能が障害され，下流遺伝子が過剰に発現することが原因と考えられてきた．しかし，最近になって，協働する因子が異なれば転写促進因子として働くことが示され，*MECP2*遺伝子変異によって下流遺伝子の発現が低下する場合もありうることが判明し，その病態は複雑である[5]．

さらに，*MECP2*領域の発現転写産物を網羅的に検討したENCODE（Encyclopaedia of DNA Elements）プロジェクトの結果をみると，近接する*IRAK1*や*OPNH1LW*遺伝子と繋がったような大きな逆向きの転写産物や，組織ごとで異なる種々の転写産物が見つかっており，それらの機能がまったくわかっていない[6]．遺伝子変異と表現型の関係は，予想された以上に複雑であることが再認識されてきている．

MECP2量の低下をもたらす*MECP2*遺伝子変異によって，Rett症候群，自閉症，Angelman類似の症候群，非症候性精神遅滞のおきることが知られているが，最近，mecp2量を正常の50％程度に低下させたマウスでは，より軽微な神経

発達学的行動異常（学習障害，巧緻運動障害，不安低下，社会性の変化，痛み反応の低下，異常な呼吸パターンなど）を認めた．これにより，ヒトにおいても*MECP2*遺伝子変異によって同様の症状が惹起される可能性が示唆されている[7]．

一方で，*MECP2*領域の重複をもち，MECP2が過剰に発現されている症例が多数報告された．その臨床的特徴は，重度精神遅滞，筋緊張低下，繰り返す呼吸器感染症，言語発達不全，けいれん，痙性などである．これらの症状のうちのいくつかは，mecp2発現を上昇させたマウスでもみられるものである[8]．これらの事実から，MECP2はその発現量が低下しても過剰になっても，精神・神経機能に大きな影響を与えることがわかる．

*ARX*に関する知見

HMGボックス型の転写因子であるARXの異常は，前述したFMRPやMECP2の場合と同様に，幅広い臨床症状と関係がある．滑脳症などの脳形成障害や生殖腺形成障害から，重症のてんかん，精神遅滞などであり，ここでも精神遅滞，てんかん，自閉症などの高次脳機能障害が一つの原因遺伝子の変異でおきることが理解できる[9]．

昨年，West症候群に加えて，大田原症候群（early infantile epileptic encephalopathy with suppression-burst pattern：EIEE）の一部は，*ARX*遺伝子のポリアラニン部位の大きなアラニンリピートの延長をもつことが報告された[10]．すでに，ARXはGABA作動性介在性ニューロンで発現することが知られており，suppression-burstとこの介在ニューロンの異常との関係が推測されている．

さらに最近，ARXのコンディショナルノックアウトマウスで，下流遺伝子として発現が変動している遺伝子を網羅的に調べた研究が報告され，*Ebf3*，*Lmo1*，*Shox2*遺伝子が，直接ARXから転写調節を受けることが判明した[11]．今後は，FMRPやMECP2と同様に，モデルマウスにおける下流遺伝子の発現を詳細にみる研究で，病態がより明らかになっていくものと期待される．

X連鎖性精神遅滞に関する話題

前述した三つの遺伝子は，いずれもX染色体上にある遺伝子であり，X連鎖性精神遅滞の原因遺伝子である．しかし，同じ遺伝子が精神遅滞ばかりでなく，てんかん，自閉症，脳形成異常などをきたすことが判明しており，これらの

表　精神遅滞研究班の結果

登録家系238家系のうち，約100家系の検査が終了した時点での陽性例のまとめ

遺伝子検査	*FMR1*	リピート延長	2家系
	ARX	リピート延長	1家系
	FTSJ1	点変異	1家系（本邦初例）
	ZNF41	点変異	1家系（本邦初例）
	PAK3	点変異	1家系（本邦初例）
	OPHN1	欠失	1家系（本邦初例）
	ARHGEF6	点変異	1家系（本邦初例）
	ATRX	点変異	2家系　ATR-X症候群疑い
	MECP2	点変異	1家系　Angelman症候群，Rett症候群疑い
	RPS6KA3	欠失	1家系　Coffin-Lowry症候群疑い
染色体検査（CGH）	X-tiling array	微小欠失	1家系
		微小重複	5家系（病的意義を検討中）
	subtelomere array	微小欠失/重複	1家系

機能解析が進むことで脳の機能発達への理解がすすみ，新たな治療戦略がみえてくる可能性がある．

一方で，精神遅滞やてんかんに関連する遺伝子は次々と同定されており，それら原因遺伝子を用いて診断を確定することは，臨床的に一定の意味のあることである．筆者らは，2003年から厚生労働省精神・神経疾患研究委託費を用いて，精神遅滞をきたす遺伝性疾患の研究を推進するための研究資源の確保と分子遺伝学研究を行ってきた．2008年9月末現在で238家系の登録があり，家系例と孤発例がほぼ同数である．そのうち，約100例の既知遺伝子解析が終了しており，表にあるような結果を得ている．やはり検査に膨大な時間と費用がかかるわりには，それぞれの遺伝子変異陽性例は1％程度であり，頻度が低い．しかしながら，陽性例はいずれもわが国では初めて発見される症例が多いこと，また陽性例の遺伝カウンセリングを行った経験から，これらの診断確定情報によって患者家族の療育態度が前向きになるなど，医療的には十分価値の高いものであることを認識した．

これらの遺伝子検査をより効率的に，より安価にできる方法を工夫すべきであり，また稀少疾患の診断にこそ遺伝子検査が有効であり，検査システムを日本の中で構築することが急務であると考えている．

文　献

1) Verkerk AJ, Pieretti M, Sutcliffe JS et al.: Identification of a gene（FMR-1）containing a CGG repeat coincident with a breakpoint cluster region exhibiting length variation in fragile X syndrome. Cell 65:905-914, 1991
2) Amiri K, Hagerman RJ, Hagerman PJ: Fragile X-associated tremor/ataxia syndrome. Arch Neurol 65: 19-25, 2008
3) Dölen G, Osterwell E, Rao BS et al.: Correction of fragile X syndrome in mice. Neuron 56:955-962, 2007
4) Wang H, Wu L-J, Kim SS et al.: FMRP acts as a key messenger for dopamine mudulation in the forebrain. Neuron 59:634-647, 2008
5) Chahrour M, Jung SY, Shaw C et al.: MeCP2, a key contributor to neurological disease, activates and represses transcription. Science 320:1224-1229, 2008
6) Singh J, Saxena A, Christodoulou J et al.: *MECP2* genomic structure and function: insights from ENCODE. Nucleic Acid Res 2008（in press）
7) Samaco RC, Fryer JD, Ren J et al.: A partial loss of function allele of methyl-CpG-biding protein 2 predicts a human neurodevelopmental syndrome. Hum Mol Genet 17:1718-1727, 2008
8) van Esch, Bauters H, Ignatis M et al.: Duplication of the *MECP2* region is a frequent cause of severe mental retardation and progressive neurological symptoms in males. Am J Hum Genet 77:442-453, 2005
9) Kato M, Das S, Petras K et al.: Mutations of ARX are associated with striking pleiotropy and consistent genotype-phenotype correlation. Hum Mutat 23: 147-159, 2004
10) Kato M, Saitoh S, Kamei A et al.: A longer polyalamnine expansion mutation in the *ARX* gene causes early infantile epileptic encephalopathy with suppression-burst pattern（Ohtahara syndrome）. Am J Hum Genet 81:361-366, 2008
11) Fulp CT, Cho G, Marsh ED et al.: Identification of Arx transcriptional targets in the developing basal forbrain. Hum Mol Genet 2008（in press）

著者連絡先

〒187-8502　東京都小平市小川東町4-1-1
国立精神・神経センター神経研究所
疾病研究第二部
後藤雄一

Journal of MEDICAL GENETICS
Home> Volume 46, Issue 9> Article

J Med Genet 2009;**46**:645-647 doi:10.1136/jmg.2008.059220

PostScript

Correspondence

A newly recognised microdeletion syndrome of 2p15-16.1 manifesting moderate developmental delay, autistic behaviour, short stature, microcephaly, and dysmorphic features: a new patient with 3.2 Mb deletion

J-S Liang[1], **K Shimojima**[1], **K Ohno**[2], **C Sugiura**[2], **Y Une**[3], **K Ohno**[2], **T Yamamoto**[1]

+ Author Affiliations

Correspondence to
Dr T Yamamoto, 8-1 Kawada-cho Shinjuku-ward Tokyo, 162-8666, Japan; yamamoto@imcir.twmu.ac.jp

Received 31 March 2008
Revised 6 April 2008
Accepted 7 April 2008

A newly recognised 2p15–16.1 microdeletion syndrome has been reported by Rajcan-Separovic *et al*.1 Their study reported two patients with 2p15–16.1 deletions of 4.5 Mb and 5.7 Mb, respectively. Subsequently, de Leeuw *et al* and Chabchoub *et al* reported new patients with deletions of 3.9 Mb and 570 Kb, respectively.2 3 The current study examines another patient with a microdeletion in the same chromosomal region.

A 4.5-year-old girl was referred to our institution because of severe psychomotor developmental delay. Due to growth obstruction during the mother's pregnancy, caesarean section was performed at 37 weeks and 6 days of gestation. Her measurements at birth were as follows: weight 2020 g (−2.7 SD); length 44 cm (−2.5 SD); head circumference 32.4 cm (−0.5 SD). Intrauterine growth retardation had been diagnosed at 24 weeks gestation. There was no asphyxic event during delivery, there were no feeding problems, and her body weight gain was within the expected range during infancy. There was no family history of 2p15–16.1 microdeletion syndrome characteristics. She was the first child of healthy parents without consanguinity.

Upon admittance, physical examination revealed growth retardation, with a height of 94 cm (−2.1 SD), a weight of 16 kg (−0.1 SD), and a head circumference of 47 cm (−2.0 SD). Dysmorphic facial features were noted, including hypertelorism, epicanthic fold, broad nasal bridge, retrognathia, and low set ears (fig 1A). Neurological examination revealed generalised muscular hypotonus and metatarsus adductovarus (fig 1B). At the time of examination, the patient could crawl but could not walk unassisted …

Genomics 94 (2009) 414–422

Contents lists available at ScienceDirect

Genomics

journal homepage: www.elsevier.com/locate/ygeno

TULIP1 (*RALGAPA1*) haploinsufficiency with brain development delay

Keiko Shimojima [a], Yuta Komoike [a,b], Jun Tohyama [c], Sonoko Takahashi [b], Marco T. Páez [a], Eiji Nakagawa [d], Yuichi Goto [d], Kousaku Ohno [e], Mayu Ohtsu [f], Hirokazu Oguni [g], Makiko Osawa [g], Toru Higashinakagawa [b], Toshiyuki Yamamoto [a,*]

[a] *International Research and Educational Institute for Integrated Medical Sciences (IREIIMS), Tokyo Women's Medical University, 8-1 Kawada-cho, Shinjuku-ward, Tokyo, 162-8666, Japan*
[b] *Department of Biology, School of Education, Waseda University, Tokyo, Japan*
[c] *Department of Pediatrics, Nishi-Niigata Chuo National Hospital, Niigata, Japan*
[d] *Department of Mental Retardation and Birth Defect Research, National Institute of Neuroscience, National Center of Neurology and Psychiatry, Tokyo, Japan*
[e] *Division of Child Neurology, Institute of Neurological Sciences, Faculty of Medicine, Tottori University, Yonago, Japan*
[f] *Department of Pediatrics, Saiseikai Yokohamashi Nanbu Hospital, Yokohama, Japan*
[g] *Department of Pediatrics, Tokyo Women's Medical University, Tokyo, Japan*

ARTICLE INFO

Article history:
Received 21 March 2009
Accepted 25 August 2009
Available online 3 September 2009

Keywords:
Chromosomal deletion
TULIP1 (RALGAPA1)
Brain
Developmental delay
Epilepsy
Human
Zebrafish

ABSTRACT

A novel microdeletion of 14q13.1q13.3 was identified in a patient with developmental delay and intractable epilepsy. The 2.2-Mb deletion included 15 genes, of which *TULIP1* (approved gene symbol: *RALGAPA1*)was the only gene highly expressed in the brain. Western blotting revealed reduced amount of TULIP1 in cell lysates derived from immortalized lymphocytes of the patient, suggesting the association between *TULIP1* haploinsufficiency and the patient's phenotype, then 140 patients were screened for *TULIP1* mutations and four missense mutations were identified. Although all four missense mutations were common with parents, reduced TULIP1 was observed in the cell lysates with a P297T mutation identified in a conserved region among species. A full-length homolog of human *TULIP1* was identified in zebrafish with 72% identity to human. Tulip1 was highly expressed in zebrafish brain, and knockdown of which resulted in brain developmental delay. Therefore, we suggest that *TULIP1* is a candidate gene for developmental delay.

Submicroscopic chromosomal aberrations are considered to comprise up to 15% of all mutations underlying monogenic diseases [1]. Microarray-based comparative genomic hybridization (aCGH) has accelerated to identify such submicroscopic genomic alterations, and many new microdeletion syndromes have been established [2]. Whereas interstitial deletion of 14q13 is rare and only a few patients have been reported. By use of aCGH analyses, we identified a unique 14q13.1q13.3 microdeletion in a patient with developmental delay and intractable epilepsy. Of the 15 genes identified in the microdeletion region, *TULIP1* (approved gene symbol: *RALGAPA1*)was the only one known to be predominantly expressed in normal brain tissue [3]. To evaluate the contribution of *TULIP1* to the patient's neurological symptoms, zebrafish embryos with morpholino knockdown system was used as a model organism [4]. Our results suggest that *TULIP1* is a candidate gene for developmental delay and epilepsy.

Results

Molecular cytogenetic analyses of 14q13.1q13.3 deletion

For patient 1 (P1), a 2.2-Mb microdeletion of 14q13.1q13.3 (33,462,439//35,694,522) was identified using aCGH (Fig. 1). Two-color fluorescent *in situ* hybridization (FISH) analysis confirmed the deletion of 14q13.1q13.3 by the loss of the RP11-26M6 and RP11-35M15 signals (Fig. 2A). Retrospective evaluation of chromosomal G-banding previously provided normal karyotype showed reasonable finding with loss of white band (Fig. 2B). FISH analysis using the same probes revealed that both parents lacked the deletion (data not shown), which indicated de novo deletion in P1. The final karyotype was arr cgh 14q13.1q13.3(33,462,439-35,694,522) ×1.ish(RP11-557O15+,RP11-26M6−,RP11-35M15−,RP11-81F13+,RP11-112H5+) de novo.

To confirm the biological parent–child relationships, microsatellite marker analysis was performed on P1 family members. The results sufficiently verified the biological relationships in this family (Supplementary Table 1) and revealed that P1 had only one peak of D14S70, which is within the deletion region; this peak was common only with the mother and there was no common peak of D14S70 with

* Corresponding author. Fax: +81 3 3352 3088.
E-mail address: yamamoto@imcir.twmu.ac.jp (T. Yamamoto).

0888-7543/$ – see front matter.
doi:10.1016/j.ygeno.2009.08.015

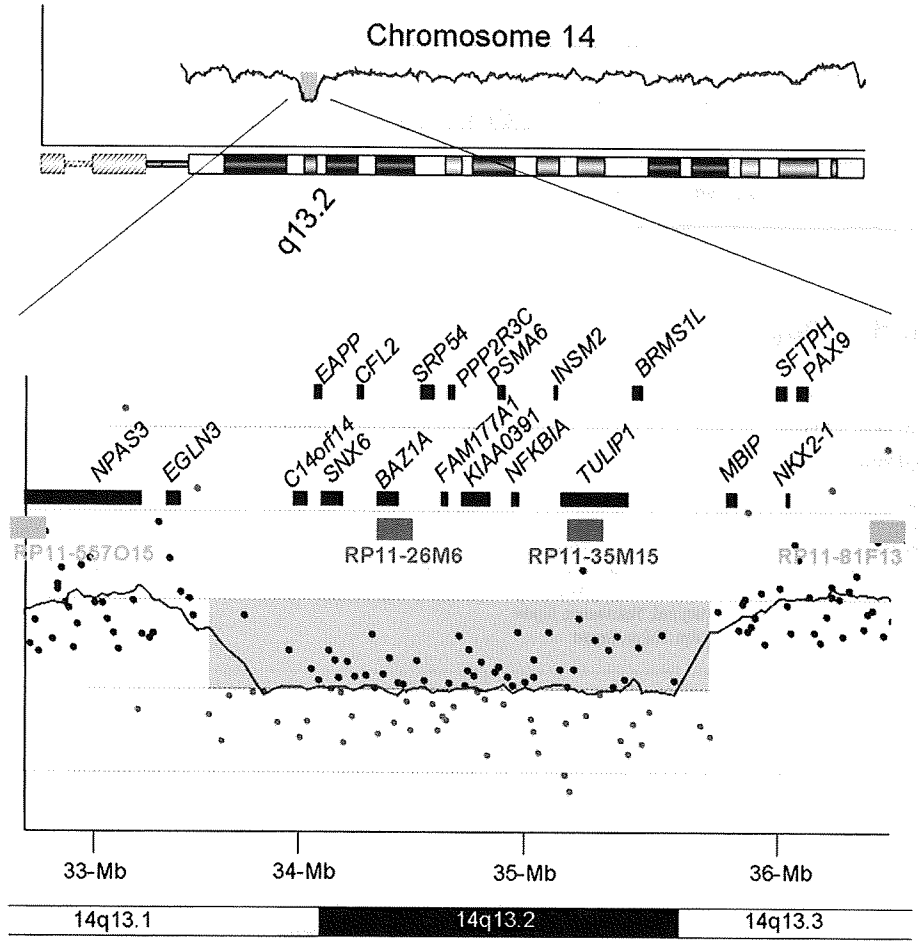

Fig. 1. The result of aCGH showing chromosomal deletion of 14q13.1q13.3 on Chromosome View (upper) and Gene View (bottom). Blue rectangles indicate the region of genomic copy number aberrations. In Gene View, the deletion region was expanded. Axial dimension indicates the physical location on chromosome 14, and vertical dimension indicates $\log_2$ ratio of intensity. Spots indicate the location of probes. Black bars indicate the locations of the known genes. Red and green bars indicate the locations of BAC clones used for FISH analyses. Italic characters indicate gene symbols.

the father (Fig. 2C). These data indicated that the paternally derived allele at this locus was deleted in P1.

Detailed clinical phenotype of P1

At the time of the study, P1 was a 7-year-old girl. Her birth weight was 3038 g and her head circumference at birth was 36 cm; there were no documented neonatal events. At 2 months, she suffered a seizure that continued for a couple of minutes; at that time she opened her eyes and both eyes and arms moved upward and were fixed. Because similar seizures occurred three times during the next 2 h, she was hospitalized. Brain computed tomography (CT) scan and electroencephalography (EEG) revealed no abnormalities. Seizures were refractory to epilepsy medication and occurred a couple of times per day. Similar to West

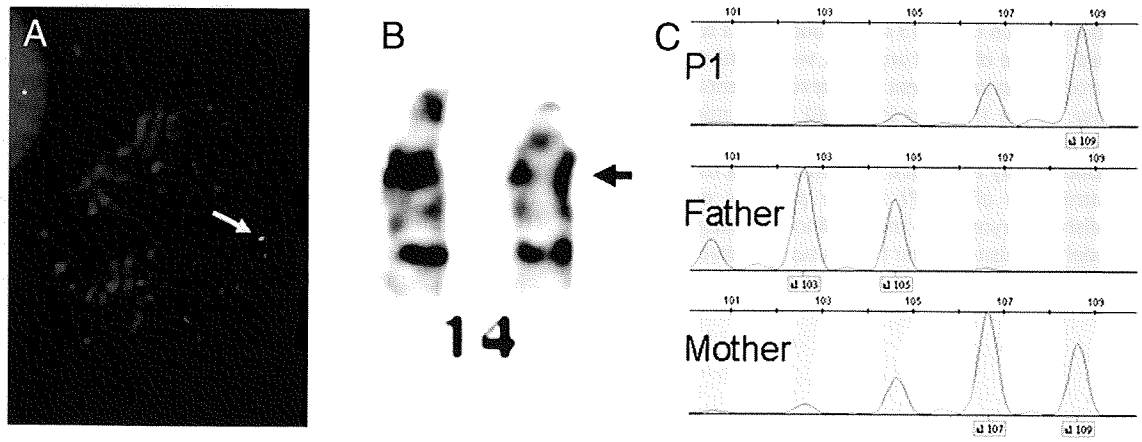

Fig. 2. Molecular cytogenetic analysis of the deletion of 14q13.1q13.3 in P1. (A) FISH analysis using RP11-112H5 (SpectrumOrange) and RP11-35M15 (SpectrumGreen) probes indicated the deletion by the loss of green signal. (B) G-banded chromosome 14 of P1 exhibited deletion of the white band (arrow). (C) GeneMapper analysis of microsatellite marker data indicated that the D14S70 band was only common to P1 and her mother (see also Supplementary Table 1).

syndrome, her seizures were composed of a series of attacks and occurred once a week after the patient reached 3 months of age.

When she was 9 months old, P1 was referred to our institution for treatment of the intractable seizures. There were no dysmorphic features. At that time, she was alert but her reaction to her surroundings was poor. Her eyes could not follow a moving target. Hypotonia was obvious but muscle power was enough to move against gravity. There was no symptom of cranial nerve damage. Tonic convulsions with eye movements and upward movement of the arms were observed intermittently. Blood screening tests, including those for inborn error of metabolism, revealed no abnormalities. The EEG showed a diffuse θ wave and a high voltage θ burst during brief tonic seizures (Supplementary Fig. 1A). However, there were no paroxysmal findings in intermittent phases. Brain magnetic resonance imaging (MRI) showed mild brain atrophy (Supplementary Fig. 1B and C). Brain single photon emission computed tomography (SPECT) showed no areas of hypoperfusion (data not shown). The results from other electrophysiological examinations, including auditory brain response (ABR), visual evoked potential (VEP), somato-sensory evoked potential (SSEP), conduction velocity (MCV), and sensory verve conduction velocity (SCV), were within normal limits (data not shown). Conventional chromosomal examination at 9 months of age indicated a normal female karyotype with 46,XX. At 5 years of age, her developmental level was evaluated using the Enjoji Scale of Infant Analytical Development (ESID) and her developmental quotient was determined to be 32 [5].

TULIP1 screening of additional patients with neurological disorders

Information regarding the genes within the deletion region of P1 was accumulated from the UCSC genome browser (http://www.genome.ucsc.edu/); 15 genes were identified in the 2.8-Mb deleted region (Fig. 1). Among the 15 genes, *TULIP1* was the only gene known to be predominantly expressed in the brain. Thus, *TULIP1* was examined as the candidate gene responsible for the clinical symptoms of P1.

Sequence analysis of the entire coding region of *TULIP1*, which contains 41 exons, was performed using originally accumulated 40 patients' samples and the 100 research resource samples. Four individual missense mutations were identified (Supplementary Fig. 2). Patient 2 (P2) had a c.889C>A nucleotide alteration in exon 9, which is predicted to result in a P297T amino acid substitution. This proband's father had the same alteration. Patient 3 (P3) and his father had a c.1055A>G (D352G) mutation in exon 10. Patient 4 (P4) and her mother had a c.1531G>A (A511T) mutation in exon 12. Patient 5 (P5) and his father had a c.3132T>G (F914C) mutation. Thus, all of the four missense mutations were inherited from healthy parents. Each of the identified missense mutations was negative in 200 normal controls. The entire coding region of *TULIP1* remaining allele of P1 was sequenced and was wild type.

P2 presented with severe mental retardation and intractable epilepsy derived from bilateral perisylvian polymicrogyria. P4 suffered West syndrome in infancy, and manifested intractable epilepsy and moderate mental retardation. P3 and P5 showed moderate mental retardation, but no epilepsy (their family trees are shown in Supplementary Fig. 3).

Analysis of TULIP1 expression

Western blotting using polyclonal rabbit anti-TULIP1 antibody was performed and reduced TULIP1 levels were confirmed in immortalized lymphocytes lysates from P1 and P2 (Fig. 3).

Identification of zebrafish tulip1

In zebrafish, a homolog of human *TULIP1* was previously predicted according to genomic information, but the gene has not yet been isolated. Therefore, we cloned and sequenced the cDNA encoding *tulip1* from zebrafish. Using RT-PCR, we identified two splice variants of *tulip1*, *tulip1.1* and *tulip1.2*, which sequences were deposited into GenBank (accession AB476643 and AB476644). The shorter variant (*tulip1.1*) consisted of 6201-bp and encoded a 2066-residue protein, and the longer variant (*tulip1.2*) was 6318-bp and encoded a 2105 residue protein. Information from the zebrafish genomic map revealed that zebrafish *tulip1* was on chromosome 17 and consisted of 41 exons. In addition, two splicing variants were identified based on alternate usage of exon 40. Although the tulip1.2 variant lacks exon 40, this variant is longer than *tulip1.1* because exon 40 contains a stop codon. This exon–intron structure and alternative splicing of exon 40 are common to human and mouse *TULIP1* [3], suggesting that *tulip1* is conserved through vertebrate evolution.

Fig. 3. Western blot analysis of TULIP1 expression. Cell lysates from immortalized lymphocytes derived from the patients indicated at the top were analyzed by Western blotting using a rabbit anti-GARNL1 (TULIP1) polyclonal antibody. P1 and P2 exhibited reduced TULIP1 expression (upper panel). β-Actin levels were evaluated as a control (lower panel).

The deduced zebrafish Tulip1.1 and Tulip1.2 protein sequences exhibited 72% identity to the corresponding splicing variants from both human and mouse, and the zebrafish splice variants each contained a Rap/Ran-GAP domain (aa 1848–aa 2027), two putative transmembrane domains (aa 1184–aa1206, aa 1370–aa1392), two putative coiled-coil motifs (aa 10–aa 37, aa 1738–aa 1770) and one leucine zipper motif (aa 1074–aa 1088), all of which are also found in human and mouse TULIP1 proteins at the same positions [3]. Collectively, these results suggested that zebrafish *tulip1.1* and *tulip1.2* are structural and functional homologs of human *TULIP1*.

To carry out *tulip1* knockdown in zebrafish using morpholino antisense oligos, precise 5′ UTR nucleotide sequence information was needed. Thus, we performed 5′ RACE to determine the sequence of the *tulip1* 5′ UTR in our zebrafish strain. Based on the obtained sequence of a 64-nucleotide fragment immediately upstream of the translational initiation site, the residue at the 5′ terminus of this sequence was guanine, whereas the residue of the position in the genomic database was cytosine. This nucleotide alteration was supposed to be the result of m7G 5′ cap structure. Therefore, this fragment means to be a full length of the 5′ UTR.

Spatial expression patterns of tulip1 during zebrafish embryonic development

To determine the spatial expression pattern of *tulip1* in zebrafish, whole-mount *in situ* hybridization of *tulip1* mRNA was performed. At the two-cell stage, *tulip1* mRNA was distributed throughout the two blastomeres (Fig. 4A), indicating that this mRNA was deposited maternally. At the shield stage, after the launch of zygotic gene expression, *tulip1* mRNA was expressed equally in whole blastomeres (Fig. 4B) and this ubiquitous expression pattern was retained during gastrulation and continued until the middle of the segmentation period (Figs. 4C and D). Later in development, distribution of *tulip1* mRNA shifted anteriorly and was restricted to the head region of embryos (Figs. 4E–G), suggesting a role for *tulip1* in zebrafish head development.

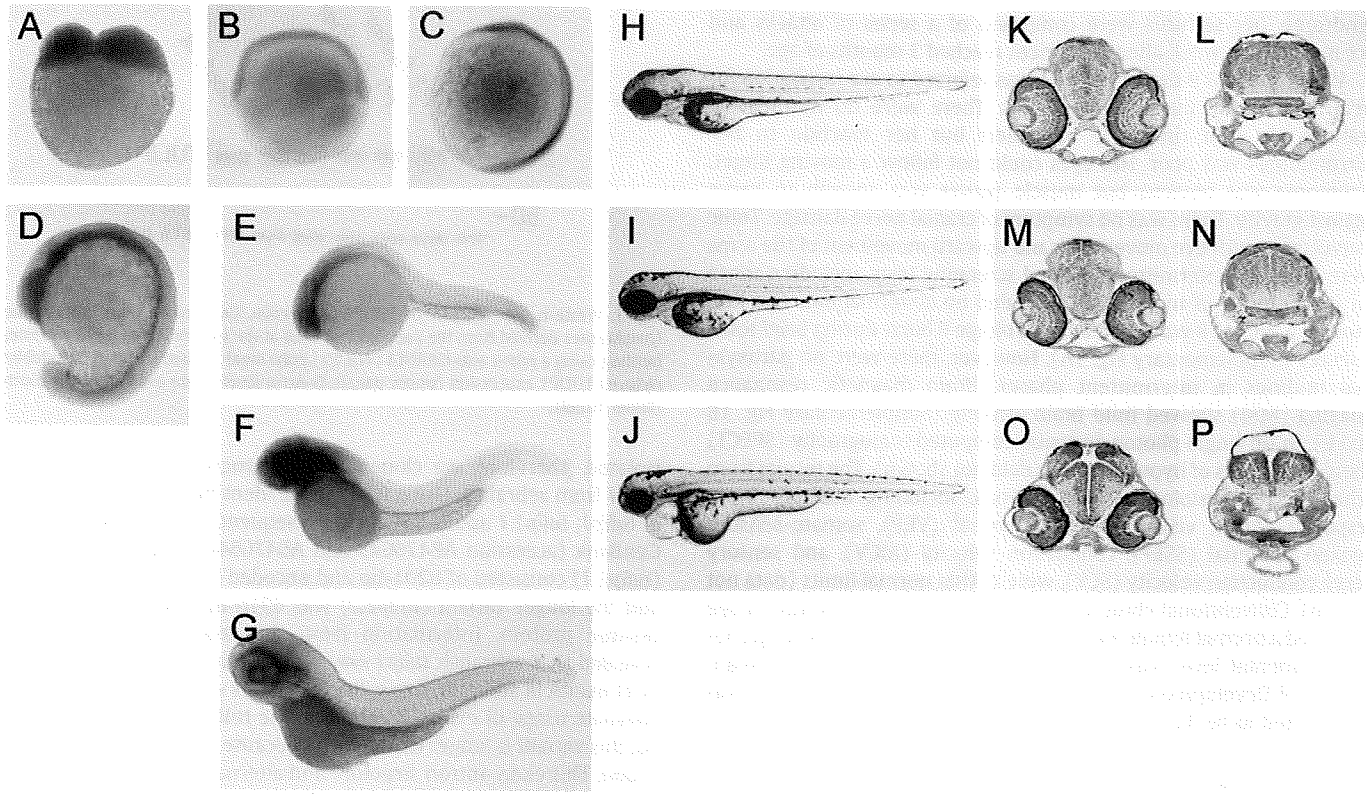

Fig. 4. Expression and functional analyses of *tulip1* in zebrafish. (A–G) *In situ* hybridization of *tulip1* mRNA during development. At the two-cell stage, *tulip1* mRNA was deposited maternally (A) and expressed ubiquitously until the middle of the segmentation period (B, shield stage; C, bud stage; D, 18 somite stage). Distribution of *tulip1* mRNA was shifted anteriorly and restricted in head region of embryos (E, 24 h post-fertilization (hpf); F, 48 hpf; G, 72 hpf). (J, O, P) Knockdown of *tulip1* caused developmental delay of the head and brain. Live whole embryos (H–J) and head cross sections corresponding to the midbrain (K, M, O) and hindbrain (L, N, P) of wild type (H, K, L), control MO-injected (I, M, N) and *tulip1* MO-injected (J, O, P) embryos at 72 hpf. Dorsal is at the top (E–P) and rostral is to the left (E–J).

Gene knockdown of tulip1 causes severe developmental retardation of the brain

To investigate whether *tulip1* is involved in brain development, we performed gene knockdown of *tulip1* in zebrafish using morpholino antisense oligos (MO). At 72 h post-fertilization (hpf), *tulip1* MO1-injected embryos (Fig. 4J) exhibited hypomorphic heads compared to wild type or control MO-injected embryos (Figs. 4H–I), whereas trunk development was relatively normal. In addition, approximately half of all morphants had an enlarged pericardium and increased yolk extension thickness (see representative morphant; Fig. 4J). To investigate whether these defects were caused by the gene-specific knockdown of *tulip1* or not, *tulip1* MO2, which is another morpholino antisense oligo and non-overlapping with *tulip1* MO1, was used. Microinjection of *tulip1* MO2 did not give rise to an enlarged pericardium and rarely caused thickening of the yolk sac (data not shown). Therefore, the heart and the yolk defects are not specific to *tulip1* knockdown. In contrast, *tulip1* MO1 and MO2 caused equivalent growth retardation of the head suggesting that this defect was caused by the specific knockdown of *tulip1* (Figs. 5A and B).

Because the externally hypomorphic head in the zebrafish morphants was similar to the abnormality of the brain observed in P1, serial sections of the head were prepared from *tulip1* MO–injected zebrafish embryos to examine specific brain morphology aberrations. In the normal zebrafish midbrain, the brain ventricle was positioned on the section that crossed the middle of the eyes at 48 hpf (Fig. 5C). This ventricle was obstructed around 60 hpf (Fig. 5E) and completely buried until 72 hpf in wild type (Fig. 4K) and control MO-injected (Fig. 4M) zebrafish. In the normal zebrafish hindbrain, the rhombic lip at 48 hpf was thin and the groove of the medulla oblongata was opened wide (Fig. 5D). The rhombic lip thickened with progressive embryonic development and, as a result, the groove of the medulla oblongata was almost fully occluded at 72 hpf in wild type (Fig. 4L) and control MO-injected (Fig. 4N) zebrafish. In contrast, in *tulip1* MO-injected embryos, the brain ventricle in the midbrain at 72 hpf was unobstructed (Fig. 4O). Similarly, a thin rhombic lip and widely opened groove of the medulla oblongata was observed in the hindbrain at 72 hpf (Fig. 4P). These results indicated that the development of the brain in *tulip1* MO-injected embryos at 72 hpf (Fig. 4O, and P) corresponded to that of the wild type embryo at 48–60 hpf (Figs. 5C–F), and suggested that *tulip1* knockdown results in brain developmental delay by $\geq$12 h (also compare Figs. 5C–D vs. H–I and compare Figs. 4K–L vs. Figs. 5J–K). Whole-body developmental delay was less severe than brain developmental delay; *tulip1* MO-injected embryos at 72 hpf were clearly as progressed as wild type embryos at 60 hpf (Fig. 5G). Collectively, these results indicated that gene knockdown of *tulip1* caused severe and specific brain developmental delay.

Discussion

Using aCGH, we identified a previously uncharacterized chromosomal deletion of 14q13.1q13.3 in a female patient with developmental delay and intractable epilepsy. Familial analysis indicated that the deletion occurred de novo. In the literature, there are at least 19 reported cases with deletions near 14q13, and the deletion identified in the present patient (P1) is the smallest among them (Fig. 6) [6–13]. Clinical findings of available 10 of these previously reported cases are summarized in Table 1. The common manifestations of the 14q13.2 deletion are developmental delay and mild microcephaly (Table 1). In the 2.2-Mb deletion in P1, 15 genes are included according to the 2006 build (Fig. 1).

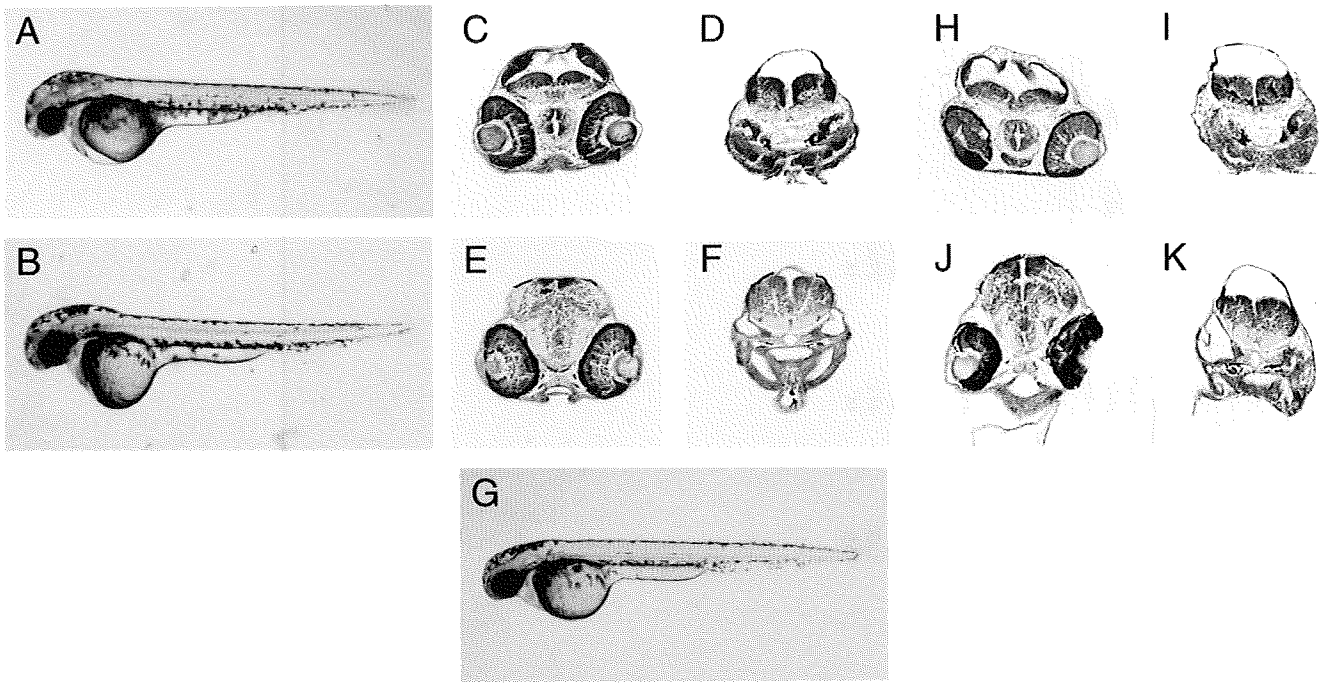

Fig. 5. *tulip1* knockdown analyses of zebrafish. Zebrafish embryos at 48 hpf injected by *tulip1* MO1 (A) and MO2 (B) showed similar hypomorphic head. Cross section of the brain of wild type (C–F) and *tulip1* MO1 embryo (H–K); midbrain (C, E, H, J) and hindbrain (D, F, I, K). Wild type embryos at 48 hpf (C, D) correspond to *tulip1* MO1 embryos at 60 hpf (H, I), and wild type embryos at 60 hpf (E, F) correspond to *tulip1* MO1 embryos at 84 hpf (J, K), which indicate developmental delay. (G) Wild type embryo at 60 hpf.

Schwarzbraun et al. considered *TULIP1* as the candidate gene for the neurological phenotypes of deletion 14q13, and analyzed the genomic structure and the function [3]. According to the study, *TULIP1* was expressed ubiquitously in pre- and postnatal human tissues. The nucleotide sequence of *TULIP1* was predicted to encode Rap–Gap domains [3], which is also contained in *TSC2*, one of the genes responsible for tuberous sclerosis. Since haploinsufficiency of *TSC2* can affects neurological functions [3], Schwarzbraun et al. analyzed the sequence of *TULIP1* in a family with idiopathic basal ganglia calcification (IBGC; Fahr disease), but found no association between

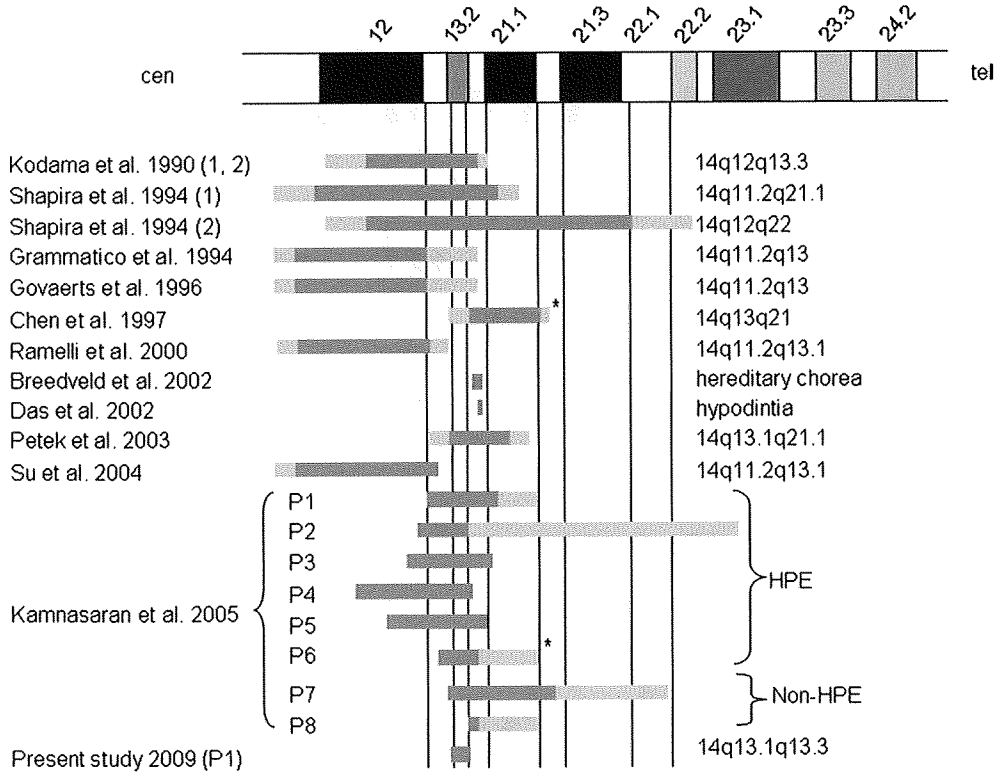

Fig. 6. Chromosome 14 schematic (upper) with the each size of deletions from previously reported patients and P1. Black and gray bars indicate confirmed and suspected deletion regions, respectively. Numbers included in parentheses indicate patient number in the reference manuscripts. Asterisks indicate results derived from the same patient. HPE: holoprosencephaly.

Table 1
Clinical information of the patients having a chromosomal deletion of 14q13q13.

	Kodama et al. 1990 (1) 14q12q13.3	Kodama et al. 1990 (2) 14q12q13.3	Shapira et al. 1994 (1) 14q11.2q21.1	Shapira et al. 1994 (2) 14q12q22	Grammatico et al. 1994 14q11.2q13	Govaerts et al. 1996 14q11.2q13	Chen et al. 1997 14q13q21	Ramelli et al. 2000 14q11.2q13.1	Petek et al. 2003 14q12q13.1	Su et al. 2004 14q11.2q13.1	Present patient 2009 14q13.1q13.3
Origin	mat	mat	pat	pat	NA	pat					pat
Pregnancy											
Oligohydramnion				–	–	–					–
Breech presentation			–		–	–					–
Duration (weeks)	41	41	39	36	38	38		40	40		36
Neonatal period											
Asphyxia		–	–	–	–	–					
Birth length (cm)	49.8	48	48	45.5	52	NA		48	55	49.5	
Birth weight (g)	3150	3150	2455	2345	3270	2370		3300	4435	2700	3038
OFC (cm)	32	32.5	31	32.5	33	30.2		33.5	34	34	36
Congenital anomalies											
Microcephaly											–
Epicanthus			NA		NA						–
Protruding upper jaw				NA	NA						–
Micrognathia					–						–
High narrow palate				NA	NA						–
Cerebral atrophy											
Corpus callosum hypoplasia					NA	–					–
Asymmetric hemisoma			–			–					–
Heart defect			NA		–	–					–
Kidney cysts			NA	NA	NA						NA
Cryptochism	female	female	female	female		–					female
Growth and development											
Growth retardation											–
Feeding problems				NA	NA						–
Arthrogryposis			NA	NA	NA						–
Hip (sub) luxation			NA			NA					–
Eye contact	–		–	–	–	–					–
Spasticity				–							–
Hypostonia			–		–	–					–
Mental retardation											
Diabetes inspidus			–	–	–						–
Renal tubrular acidosis				–	–	–					–
Reccurent infections				NA	NA						–

mat, maternally derived; pat, paternally derived; NA, not available.

TULIP1 mutation and idiopathic basal ganglia calcification. Whereas, the similarities between *TULIP1* and *TSC2* led us to hypothesize that *TULIP1* might be associated with the idiopathic developmental delay and epilepsy.

In the present study, reduced TULIP1 levels were observed in cell lysates from immortalized lymphocytes derived from P1 (Fig. 3). Subsequent mutation analyses identified no *TULIP1* mutation on the remaining allele. This evidence indicates that *TULIP1* expression is allele-dose dependent, making *TULIP1* a credible candidate gene for the phenotype of P1. We therefore analyzed the entire *TULIP1* coding region from 140 subjects with developmental delay and/or epilepsy. From this second screening, four individual *TULIP1* missense mutations were identified in four patients (Supplementary Fig. 2), and two of them were located within conserved sequence region among mammalian species (Supplementary Fig. 4). However, all four missense mutations were inherited from their healthy parents (Supplementary Figs. 2 and 3).

To confirm whether *TULIP1* deletion influenced the phenotypic appearance of P1, we used a zebrafish knockdown system in which expression of the zebrafish homolog of *TULIP1* was artificially depressed. We first identified and sequenced the full-length cDNA of zebrafish *tulip1* including the 5′ and 3′ UTRs; the zebrafish and human sequences shared 72% identity. *In situ* hybridization revealed that Tulip1 was expressed in the wild type zebrafish forebrain and *tulip1* knockdown resulted in brain developmental delay but normal whole body development. These findings are comparable to that observed for P1, who had *TULIP1* deletion and manifested severe developmental delay, intractable epilepsy, and mild cerebral atrophy.

Kamnasaran et al. reported six patients associated with holoprosencephaly and common 14q13 microdeletion, which is overlapped with that of the present patient (P1) (Fig. 6) [14]. In spite of common deletions, penetrance of holoprosencephaly was not 100%, which may depend on the parental origin of the deletion. Uniparental disomy of chromosome 14 (UPD14) results in a distinctive phenotype with developmental delay and dysmorphic features depending on the parental origin [15,16]. Although the imprinting locus of UPD14 is far from the 14q13 locus, we cannot deny the possibility that penetrance of holoprosencephaly is influenced by the allele origin.

As same as this manner, *TULIP1* may be influenced by genomic imprinting. Although the missense mutation P297T was shared with P2 and her healthy father, western blotting analyses showed reduced TULIP1 expression in immortalized lymphocyte cell extracts from P2. If *TULIP1* was transcribed only from the paternal allele, P2 would only be able to synthesize the mutated protein [17]. The evidence that chromosomal deletion of 14q13.q13.3 in P1 was derived from paternal allele may support this hypothesis. Therefore, we cannot rule out possible pathogenicity of familial missense mutations identified in this study.

Materials and methods

Materials

After informed consent based on the permission of the ethical committee of Tokyo Women's Medical University, peripheral blood samples of 300 patients with idiopathic mental retardation and/or epilepsy of unidentified etiology were accumulated to investigate potential genomic copy number aberrations using aCGH. In some cases of chromosomal aberrations, blood samples were also obtained from both parents of the patient. The samples in which no genomic copy number aberrations were identified were used in the second screening to identify whether gene-specific mutations were present. In this study, 40 samples derived from patients with neurological symptoms including developmental delay and/or epilepsy were used for the second screening. An additional 100 subjects, which were determined by aCGH to be negative for chromosomal aberrations and other known disease-causing mutations, including mutation of *FMR1*, *AFF2*, *PQBP1*, *ARX*, *MECP2*, *ATRX*, *RPS6KA3*, *IL1RAPL1*, *TSPAN7*, *OPHN1*, *PAK3*, *ACSL4*, *AGTH2*, *ARHGEF6*, *GDI1*, *SLC6A8*, *FTSJ1*, *ZNF41*, and *DLG3*, were provided by the consortium of Research Resource for Mental Retardation supported by the Ministry of Welfare, Labor, and Health of Japan [18]. One hundred DNA samples from peripheral blood lymphocyte of healthy Japanese volunteers and one hundred Caucasian DNA samples (Caucasian Panel of 100 (HD100CAU); Coriell Institute for Medical Research, USA) were also used for the population study.

aCGH analysis

Genomic DNA was extracted from peripheral blood using the QIA quick DNA extraction kit (Qiagen, Hilden, Germany). Genomic copy number aberrations were analyzed using the Human Genome CGH Microarray 105A chip (Agilent Technologies, Santa Clara, CA) according to the method described elsewhere [19–22]. Briefly, 500 ng patient and reference DNA from healthy Japanese individuals were digested with restriction enzymes, Alu I and RsaI (Promega, Madison, WI). Cy-5 (patient) or Cy-3 dUTP (reference) were incorporated using Klenow fragment. The array was hybridized with labeled patient and reference DNA in the presence of Cot-1 DNA (Invitrogen, Carlsbad, CA) and blocking agents (Agilent Technologies) for 40 h at 65 °C, washed and scanned on the scanner (Agilent Technologies). Data was extracted using Agilent Feature Extraction software ver 9 with the default settings for aCGH analysis. Statistically significant aberrations were determined using the ADM-II algorithm in CGH Analytics software version 3.5 (Agilent Technologies). Breakpoints were defined as the start and stop location of the first and last probes, respectively, included in the algorithmically determined region of deletion.

Fluorescence in situ hybridization (FISH) analysis

Metaphase or prometaphase chromosomes were prepared from phytohemagglutinin-stimulated peripheral blood lymphocytes according to standard techniques. Four bacterial artificial chromosome (BAC) clones RP11-557O15 (14q13.1; 32,770,543//32,934,772), RP11-26M6 (14q13.2; 34,404,823//34,591,592), RP11-35M15 (14q13.2; 35,104,496//35,263,440) and RP11-81F13 (14q13.3; 36,297,744//36,467,869) that mapped around 14p13.2 were selected from the in-silico library build 2006 (UCSC Human genome browser, March 2006, http://genome.ucsc.edu/) and were purchased from Invitrogen (Germany). Clone RP11-112H5 (14q32.33; 105,798,044//105,952,495) was used for the marker of chromosome 14.

FISH analyses were performed using a combination of two BAC clones with the target clone and the marker clone [22]. Briefly, slide-mounted chromosomes were hardened at 65 °C for 150 min and then denatured in 70% formamide containing 2× standard saline citrate (SSC) at 70 °C for 2 min, and then dehydrated at −20 °C in ethanol. 1.5 μg of BAC clone DNA extracted using GenePrepStar PI-80X (Kurabo, Osaka, Japan) was labeled with SpectrumGreen TM-11-dUTP or SpectrumOrange TM-11-dUTP (Vysis, Downers Grove, IL) via nick translation and denatured at 70 °C for 5 min in the probe hybridization mixture including 50% of formamide, 2×SSC, and 10% dextran sulfate. Then, it was applied on the chromosomes, and incubated at 37 °C for 16 h. Slides were washed twice in 50% formamide containing 2×SSC at 43 °C for 15 min, 2×SSC for 5 min, 1×SSC for 5 min, 0.1% (v/v) Triton X-100/4×SSC for 5 min with shaking, 4×SSC for 5 min, then 2×SSC for 5 min and then mounted in antifade solution (Vector, Burlingame, CA) containing 4′,6-diamino-2-phenylindole (DAPI). Photomicroscopy was performed under a microscope equipped with a quad filter set containing single band excitation filters (Leica Microsystems, Tokyo, Japan).

Microsatellite marker analysis

Familial relationships and the origin of the 14q13.1q13.3 deletion for P1 were analyzed using the PRISM Linkage Mapping Set Panel 20 (Applied Biosystems Inc, Foster City, CA), which includes the primer sets of 14 microsatellite markers D14S261, D14S283, D14S275, D14S70, D14S288, D14S276, D14S63, D14S258, D14S74, D14S68, D14S280, D14S65, D14S985 and D14S292. PCR amplification using True Allele PCR Premix (Applied Biosystems Inc.) was performed according to the manufacture's protocol [23]. Then, the products were separated using the 3130xl Genetic Analyzer (Applied Biosystems Inc.) and analyzed by GeneMapper software (Applied Biosystems Inc.).

Mutation screening of the TULIP1 coding region

All 41 *TULIP1* exons from each patient were amplified by PCR using originally designed primers located on the both neighboring intronic sequences (Supplementary Table 2) according to the standard method. All amplicons were subjected to direct sequencing using the BigDye Terminator Cycle Sequencing kit (Applied Biosystems Inc.) according to the manufacturer's protocol. Sequencing reactions were separated using a 3130xl Genetic Analyzer (Applied Biosystems Inc.).

Because exon 33 was too large to analyze in the same manner with the other exons, it was divided into several parts. However, primers based on the exonic sequence could not be used for PCR due to the existence of the pseudogene of *TULIP1* which had quite similar sequences. When we use the primers on the coding region of exon 33 for PCR amplification, both the true *TULP1* and pseudo *TULIP1* were amplified. To circumvent this difficulty, the entire exon 33 was PCR amplified by both neighboring intron-based primers, which cannot amplify exon 33 of the pseudogene of *TULIP1*, and used as a template for direct sequencing using sequential exon-based primers.

Western blotting

Immortalized lymphocytes were collected by centrifugation at 1400 × *g* and homogenized in sample buffer (50 mM Tris–HCl, pH 6.8, 2% sodium dodecyl sulfate (SDS), and 10% (v/v) glycerol) by sonication. β-Mercaptoethanol and bromophenol blue were added to cell lysates at final concentrations of 6% (v/v) and 0.003%, respectively. Proteins were resolved by SDS-PAGE and transferred to polyvinylidene difluoride membranes (Immobilon; Millipore, Billerica, MA). Membranes were blocked in phosphate buffered saline (PBS) containing 10% nonfat milk and 0.05% (w/v) Tween 20 for 1 h at room temperature. Membranes were then incubated with rabbit polyclonal anti-GARNL1 (TULIP1) (1:100 dilution, HPA00851; Atlas Antibodies, Sweden) or anti-β-actin monoclonal antibody (1:5000 dilution, A5441; Sigma, MO) overnight at 4 °C. Membranes were washed three times in PBS containing 0.05% Tween 20 and then incubated in HRP-conjugated secondary antibody for 1 h at 37 °C. Membranes were washed as before and signals were detected using SuperSignal West Pico Chemiluminescent Substrate (Thermo Fisher Scientific Inc., Rockford, IL) and FUJI RAS3000 (FUJI Film, Tokyo, Japan).

Zebrafish maintenance

Adult zebrafish (*Danio rerio*) were maintained at 28.5 °C under 14 h light/10 h dark cycle conditions. Embryos from natural crosses were collected a few minutes after spawning and cultured at 28.5 °C in water containing 0.006% NaCl and 0.00025% methylene blue. Embryos were staged according to morphology and hours post-fertilization (hpf) as described [4]. For *in situ* hybridization, *N*-phenylthiourea was added to culture water at a final concentration of 0.003% to avoid pigmentation of larvae.

Cloning of zebrafish tulip1

The sequence of the zebrafish tulip1 cDNA has been previously predicted using genomic data (GenBank accession XM_679242). In this study, the cDNA corresponding to the open reading frame (ORF) of *tulip1* was cloned by reverse transcription-polymerase chain reaction (RT-PCR) using primers designed based on the predicted sequence. Briefly, total RNA was extracted from 14 somite stage embryos using the RNeasy Mini Kit (Qiagen), and cDNA was synthesized using the Omniscript RT Kit (Qiagen) according to the manufacturer's instructions. All PCR amplification reactions were performed using KOD plus DNA polymerase (TOYOBO, Osaka, Japan). The 5′ and 3′ untranslated regions were also cloned by the rapid amplification of cDNA ends (RACE) method using the 5′-RACE Core Set (TAKARA, Otsu, Japan). (The sequences of the primers used in this study are shown in Supplementary Table 3.)

Whole mount in situ hybridization of tulip1 RNA

Whole-mount *in situ* hybridization was performed as described [4]. Briefly, digoxigenin-labeled antisense RNA probes, complementary to four partially overlapping regions of zebrafish *tulip1*, were synthesized. These probes corresponded to the following regions of *tulip1*; nt 511–1526, nt 1303–2337, nt 3714–4733 or nt 4527–5644 (relative the transcriptional start site GenBank accession AB476643 and AB476644). Because these four probes displayed identical staining patterns, they were used as a mixture. To enhance the contrast of the signal of *tulip1* in shield and bud stage embryos, specimens were soaked in transparency reagent (2:1 mixture of benzyl benzonate/benzyl alcohol).

Morpholino oligos and microinjection

Morpholino antisense oligos (MOs) were purchased from Gene Tools, LLC. The sequences of the two non-overlapping MOs used in this study were as follows: *tulip1* MO1, 5′-GAGATGTTTTGAAGAGCTAATGATA-3′; *tulip1* MO2, 5′-TCTTCCGTTAATTCCCTCAAACATG-3′. We also used the following control MO that does not match any zebrafish gene: 5′-AAACGTCTCTTGACTCTCCGCGATG-3′. MOs were dissolved in Danieau solution (5 mM HEPES, pH 7.6, 58 mM NaCl, 0.7 mM KCl, 0.4 mM $MgSO_4$, and 0.6 mM $Ca(NO_3)_2$) to a final concentration of at 10 μg/μl and stored at −20 °C. MOs were microinjected at 3 ng/nl as described [4].

Preparation of zebrafish head sections

Zebrafish embryos in appropriate stages were fixed in PBS containing 4% paraformaldehyde (PFA) at 4 °C overnight. The fixed embryos were gradually dehydrated with ethanol and then completely dehydrated using 2-propanol. Dehydrated embryos were soaked in xylene and embedded following transfer to Paraplast Plus embedding medium (McCormick Scientific, St. Louis, MO) under microscopic observation. Specimens were cut into serial sections (7 μm) and stained using Mayer's hematoxylin and eosin solutions.

Acknowledgment

This work was supported by the International Research and Educational Institute for Integrated Medical Sciences, Tokyo Women's Medical University, which is supported by the Program for Promoting the Establishment of Strategic Research Centers, Special Coordination Funds for Promoting Science and Technology, Ministry of Education, Culture, Sports, Science and Technology (Japan).

Appendix A. Supplementary data

Supplementary data associated with this article can be found, in the online version, at doi:10.1016/j.ygeno.2009.08.015.

References

[1] L.E. Vissers, J.A. Veltman, A.G. van Kessel, H.G. Brunner, Identification of disease genes by whole genome CGH arrays, Hum. Mol. Genet. 14 (Spec No. 2) (2005) R215–223.

[2] A.M. Slavotinek, Novel microdeletion syndromes detected by chromosome microarrays, Hum. Genet. 124 (2008) 1–17.

[3] T. Schwarzbraun, J.B. Vincent, A. Schumacher, D.H. Geschwind, J. Oliveira, C. Windpassinger, L. Ofner, M.K. Ledinegg, P.M. Kroisel, K. Wagner, E. Petek, Cloning, genomic structure, and expression profiles of TULIP1 (GARNL1), a brain-expressed candidate gene for 14q13-linked neurological phenotypes, and its murine homologue, Genomics 84 (2004) 577–586.

[4] M.A. Razzaque, T. Nishizawa, Y. Komoike, H. Yagi, M. Furutani, R. Amo, M. Kamisago, K. Momma, H. Katayama, M. Nakagawa, Y. Fujiwara, M. Matsushima, K. Mizuno, M. Tokuyama, H. Hirota, J. Muneuchi, T. Higashinakagawa, R. Matsuoka, Germline gain-of-function mutations in RAF1 cause Noonan syndrome, Nat. Genet. 39 (2007) 1013–1017.

[5] T. Hokama, M. Gushi Ken, N. Nosoko, Iron deficiency anaemia and child development, Asia Pac. J. Public Health 17 (2005) 19–21.

[6] M. Kodama, Y. Kai, S. Sugino, N. Inokuchi, T. Miike, Two siblings with interstitial deletion of chromosome 14 [46 XX, del (14) (q12 q13.3)], No To Hattatsu (in Japanese) 22 (1990) 61–65.

[7] S.K. Shapira, K.L. Anderson, A. Orr-Urtregar, W.J. Craigen, J.R. Lupski, L.G. Shaffer, De novo proximal interstitial deletions of 14q: cytogenetic and molecular investigations, Am. J. Med. Genet. 52 (1994) 44–50.

[8] P. Grammatico, S. de Sanctis, C. di Rosa, F. Cupilari, G. del Porto, First case of deletion 14q11.2q13: clinical phenotype, Ann. Genet. 37 (1994) 30–32.

[9] L. Govaerts, J. Toorman, M.V. Blij-Philipsen, D. Smeets, Another patient with a deletion 14q11.2q13, Ann. Genet. 39 (1996) 197–200.

[10] C.P. Chen, C.C. Lee, L.F. Chen, C.Y. Chuang, S.W. Jan, B.F. Chen, Prenatal diagnosis of de novo proximal interstitial deletion of 14q associated with cebocephaly, J. Med. Genet. 34 (1997) 777–778.

[11] G.P. Ramelli, L. Remonda, K.O. Lovblad, H. Hirsiger, H. Moser, Abnormal myelination in a patient with deletion 14q11.2q13.1, Pediatr. Neurol. 23 (2000) 170–172.

[12] E. Petek, B. Plecko-Startinig, C. Windpassinger, H. Egger, K. Wagner, P.M. Kroisel, Molecular characterisation of a 3.5 Mb interstitial 14q deletion in a child with several phenotypic anomalies, J. Med. Genet. 40 (2003) e47.

[13] P.H. Su, S.J. Chen, I.C. Lee, K.L. Wang, J.Y. Chen, H.M. Hung, C.F. Lee, Interstitial deletion of chromosome 14q in a Taiwanese infant with microcephaly, J. Formos Med. Assoc. 103 (2004) 385–387.

[14] D. Kamnasaran, C.P. Chen, K. Devriendt, L. Mehta, D.W. Cox, Defining a holoprosencephaly locus on human chromosome 14q13 and characterization of potential candidate genes, Genomics 85 (2005) 608–621.

[15] M. Kagami, Y. Sekita, G. Nishimura, M. Irie, F. Kato, M. Okada, S. Yamamori, H. Kishimoto, M. Nakayama, Y. Tanaka, K. Matsuoka, T. Takahashi, M. Noguchi, Y. Tanaka, K. Masumoto, T. Utsunomiya, H. Kouzan, Y. Komatsu, H. Ohashi, K. Kurosawa, K. Kosaki, A.C. Ferguson-Smith, F. Ishino, T. Ogata, Deletions and epimutations affecting the human 14q32.2 imprinted region in individuals with paternal and maternal upd(14)-like phenotypes, Nat. Genet. 40 (2008) 237–242.

[16] T. Ogata, M. Kagami, A.C. Ferguson-Smith, Molecular mechanisms regulating phenotypic outcome in paternal and maternal uniparental disomy for chromosome 14, Epigenetics 3 (2008) 181–187.

[17] S. Saitoh, T. Wada, Parent-of-origin specific histone acetylation and reactivation of a key imprinted gene locus in Prader-Willi syndrome, Am. J. Hum. Genet. 66 (2000) 1958–1962.

[18] K. Takano, E. Nakagawa, K. Inoue, F. Kamada, S. Kure, Y. Goto, A loss-of-function mutation in the FTSJ1 gene causes nonsyndromic X-linked mental retardation in a Japanese family, Am. J. Med. Genet. B Neuropsychiatr. Genet. 147B (2008) 479–484.

[19] M.T. Barrett, A. Scheffer, A. Ben-Dor, N. Sampas, D. Lipson, R. Kincaid, P. Tsang, B. Curry, K. Baird, P.S. Meltzer, Z. Yakhini, L. Bruhn, S. Laderman, Comparative genomic hybridization using oligonucleotide microarrays and total genomic DNA, Proc. Natl. Acad. Sci. U. S. A. 101 (2004) 17765–17770.

[20] A. Bartocci, P. Striano, M.M. Mancardi, M. Fichera, L. Castiglia, O. Galesi, R. Michelucci, M. Elia, Partial monosomy Xq(Xq23→qter) and trisomy 4p (4p15.33→pter) in a woman with intractable focal epilepsy, borderline intellectual functioning, and dysmorphic features, Brain Dev. 30 (2008) 425–429.

[21] G.A. Toruner, D.L. Streck, M.N. Schwalb, J.J. Dermody, An oligonucleotide based array-CGH system for detection of genome wide copy number changes including subtelomeric regions for genetic evaluation of mental retardation, Am. J. Med. Genet. A 143A (2007) 824–829.

[22] K. Shimojima, M. Adachi, M. Tanaka, Y. Tanaka, K. Kurosawa, T. Yamamoto, Clinical features of microdeletion 9q22.3 (pat), Clin. Genet. 75 (2009) 384–393.

[23] K. Shimojima, K. Tanaka, T. Yamamoto, A de novo intra-chromosomal tandem duplication at 22q13.1q13.31 including the Rubinstein-Taybi region but with no bipolar disorder, Am. J. Med. Genet. A 149A (2009) 1359–1363.

Epilepsy Research (2010) 89, 303–309

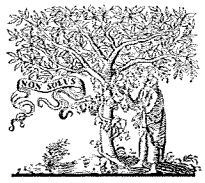

ELSEVIER

journal homepage: www.elsevier.com/locate/epilepsyres

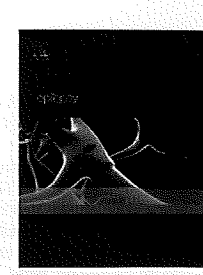

Genomic copy number variations at 17p13.3 and epileptogenesis

Keiko Shimojima[a], Chitose Sugiura[b], Hiroka Takahashi[c], Mariko Ikegami[c], Yukitoshi Takahashi[c], Kousaku Ohno[b], Mari Matsuo[d], Kayoko Saito[d], Toshiyuki Yamamoto[a,*]

[a] *International Research and Educational Institute for Integrated Medical Sciences (IREIIMS), Tokyo Women's Medical University, Tokyo, Japan*
[b] *Division of Child Neurology, Institute of Neurological Science, Faculty of Medicine, Tottori University, Yonago, Japan*
[c] *National Epilepsy Center, Shizuoka Institute of Epilepsy and Neurological Disorders, Shizuoka, Japan*
[d] *Institute of Medical Genetics, Tokyo Women's Medical University, Tokyo, Japan*

Received 9 December 2009; received in revised form 4 February 2010; accepted 11 February 2010
Available online 12 March 2010

KEYWORDS
17p13.3;
Array comparative genomic hybridization (array CGH);
LIS1;
YWHAE;
Fluorescent *in situ* hybridization (FISH);
Epileptogenesis

Summary Deletion of the terminal end of 17p is responsible for Miller-Dieker syndrome (MDS), which is characterized by lissencephaly, distinctive facial features, growth deficiency, and intractable seizures. Using microarray-based comparative genomic hybridization, 3 patients with epilepsy were revealed to have genomic copy number aberrations at 17p13.3: a partial *LIS1* deletion in a patient with isolated lissencephaly and epilepsy, a triplication of LIS1 in a patient with symptomatic West syndrome, and a terminal deletion of 17p including *YWHAE* and *CRK* but not *LIS1* in a patient with intractable epilepsy associated with distinctive facial features and growth retardation. In this study, it was suggested that the identified gain or loss of genomic copy numbers within 17p13.3 result in epileptogenesis and that triplication of *LIS1* can cause symptomatic West syndrome.

Introduction

The terminal end of the short arm of chromosome 17 is crucial for neurodevelopment and deletion of this region is associated with Miller-Dieker syndrome (MDS), a congenital malformation syndrome consisting of typical lissencephaly and distinctive facial features. Patients with MDS also show growth deficiency, severe developmental delays, and intractable seizures (Dobyns et al., 1991). MDS results from chromosomal disruption, including cytogenetically visible or submicroscopic deletions of the 17p13.3 region, which includes *LIS1*, a key indicator of MDS (Dobyns et al., 1993; Reiner et al., 1993). *LIS1* encodes PAFAH1B1 and participates in neural migration, disruption of which is responsible for lissencephaly. Indepen-

* Corresponding author at: International Research and Educational Institute for Integrated Medical Sciences (IREIIMS), Tokyo Women's Medical University, 8-1 Kawada-cho, Shinjuku-ward, Tokyo 162-8666, Japan. Tel.: +81 3 3353 8111x24067; fax: +81 3 3352 3088.
E-mail address: yamamoto@imcir.twmu.ac.jp (T. Yamamoto).

0920-1211/$ – see front matter © 2010 Elsevier B.V. All rights reserved.
doi:10.1016/j.eplepsyres.2010.02.002

dent *LIS1* deletions or nucleotide alterations in its coding exons cause isolated lissencephaly without growth deficiency or distinctive facial features (Cardoso et al., 2000). This finding indicates that the clinical manifestations associated with MDS patients, such as growth deficiency and dysmorphic features, are likely derived from other genes included in the 17p13.3 region. Genotype–phenotype correlation studies in patients with deletions in the terminal region of 17p revealed that *LIS1* deletion is responsible for lissencephaly and that combined deletion of *LIS1* and *YWHAE* results in severer lissencephaly and a distinctive facial appearance, the hallmarks of MDS (Cardoso et al., 2003).

Recent revolutionary technological advances in molecular cytogenetics have enabled us to identify submicroscopic chromosomal abnormalities including gain or loss of genomic copy numbers (Emanuel and Saitta, 2007). Such genomic copy number variations (CNV) have only recently been identified using microarray-based comparative genomic hybridization (aCGH), and the incidence of such abnormalities seems to be more frequent than was thought prior to the human genome project (Shaffer et al., 2007). Genomic duplications are of particular interest because many submicroscopic duplications have been shown to be related to neurological disorders, including developmental delay and epilepsy (Lee and Lupski, 2006). Small genomic deletions and duplications have also been reported in 17p13.3 (Bi et al., 2009; Haverfield et al., 2009; Mei et al., 2008; Mignon-Ravix et al., 2009; Roos et al., 2009; Sreenath Nagamani et al., 2009).

In this study, we identified three types of genomic CNVs in the chromosome 17p13.3 region in 3 patients with epilepsy. This result implicates the dose effects of the genes in the 17p terminal region in epilepsy.

Materials

After obtaining informed consents from the patients' families based on the permission approved by the ethical committee of the institution, peripheral blood samples were obtained from 300 patients with psychomotor developmental delay and/or epilepsy, which included 10 patients with early infantile epileptic encephalopathy, 43 patients with West syndrome, 2 patients with Lennox-Gastaut syndrome, 12 patients with symptomatic generalized epilepsy, 14 patients with symptomatic partial epilepsy, and 5 patients with other types of epilepsy.

Methods

aCGH analysis was performed using the Human Genome CGH Microarray 105A chip (Agilent Technologies, Palo Alto, CA, USA), according to the manufacturer's protocol (Shimojima et al., 2009). Genomic DNAs were extracted from peripheral blood using a QIAquick DNA extraction kit (Qiagen, Hilden, Germany), and genomic copy numbers were determined using CGH Analytics software version 3.5 (Agilent Technologies).

To confirm the genomic copy number variations identified by aCGH, fluorescent *in situ* hybridization (FISH) analysis was performed as described (Shimojima et al., 2009). To confirm whether the identified genomic copy number variations were de novo or not, parental samples were also obtained and analyzed.

The wild-type genomic sequence of *LIS1* exons 9–11 was amplified by long PCR using LA-Taq (Takara, Otsu, Japan), a forward primer designed to anneal within intron 8 (5′-CAGTGCTGTGCTATAACTGCACTATC-3′), and a reverse primer designed to anneal within exon 9 (5′-CACTGGCAGGTGTATACTATCAGATAC-3′), according to the manual provided by the manufacture. Then, the 2867-bp amplicon was cloned into the p-GEM T-vector® (Promega, Madison, WI, USA), and the resulting plasmid was used as a probe for FISH analysis. The bacterial artificial chromosome (BAC) clones mapped to chromosome 17p13.3 (Table 1) were selected from an in silico library (UCSC Human Genome Browser, March 2006, http://genome.ucsc.edu).

Fiber-FISH analysis was performed to determine the directionality of the repeated segments as described elsewhere (Shimojima et al., 2009).

Results

Molecular and cytogenetic analysis

In patient 1, a loss of genomic copy number was identified by aCGH. The deletion was comprised of a 294-kb region of chr17 (2,522,672–2,816,939), including the last 5 exons of *LIS1* (exons 7–11) and the neighboring *KIAA0664* and *GARNL* (Fig. 1). FISH analysis using an originally cloned plasmid probe containing the predicted deletion sequence confirmed the deletion of one copy of *LIS1* (Fig. 2A). The fact that neither parent had the *LIS1* deletion (data not shown) confirmed it as a de novo deletion in patient 1.

Table 1 Summary of FISH analyses.

Clone	Band	Start[a]	End[a]	Patient 1	Patient 2	Patient 3	Coverage genes
RP11-629C16	17p13.3	373,082	560,333	NT	NT	Deletion	
RP11-356I18	17p13.3	707,755	880,135	NT	NT	Deletion	
RP11-294J5	17p13.3	1,146,211	1,299,309	NT	NT	Deletion	*YWHAE, CRK*
RP11-380H7	17p13.3	2,026,967	2,250,500	NT	Duplication	NT	
RP11-135N5	17p13.3	2,312,022	2,492,178	NT	Triplication	NT	*LIS1*
CTD-2576K4	17p13.3	2,492,176	2,643,505	NT	Triplication	NT	*LIS1*
Plasmid[b]	17p13.3	2,528,949	2,530,730	Deletion	NT	NT	*LIS1*
RP11-1D5	17p13.1	7,918,567	8,082,208	Marker	Marker	NT	
RP11-153A23	17q25.3	73,516,547	73,694,284	NT	NT	Marker	

NT: not tested.
[a] Genomic position is according to the May 2006 human reference sequence (Build 2006).
[b] Originally constructed plasmid probe.

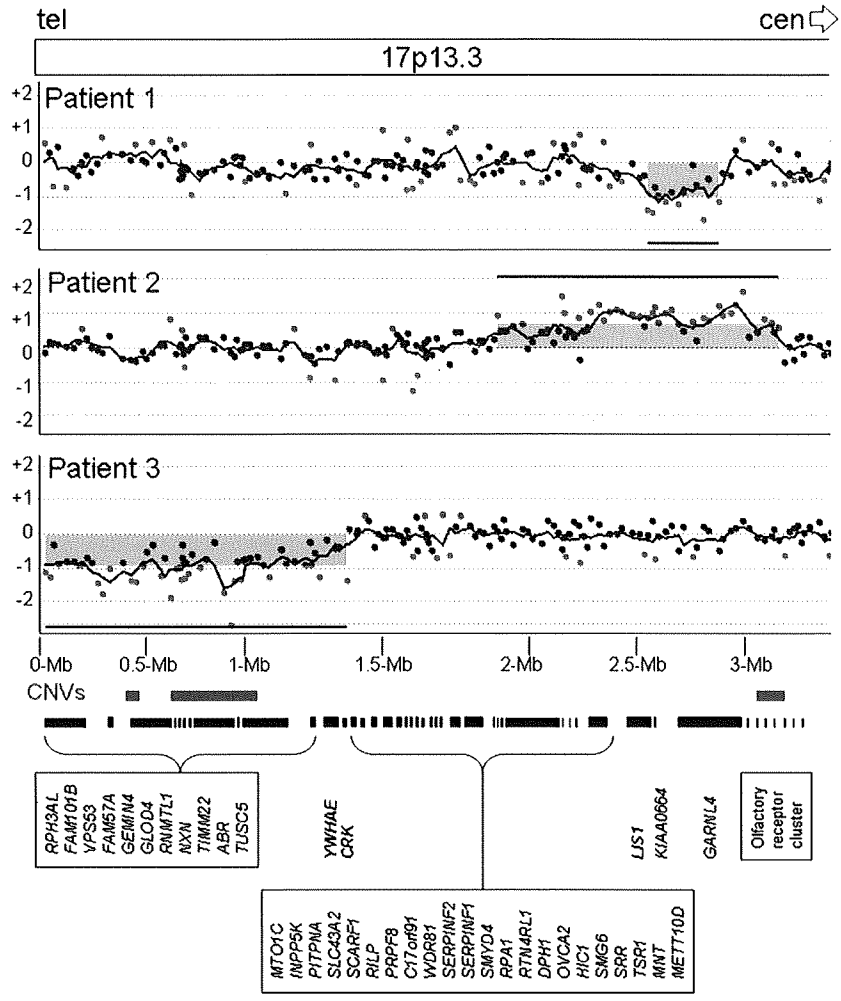

Figure 1 aCGH analysis of the 17p13.3 region in 3 epilepsy patients and a corresponding genetic map of the MDS region. Genomic copy number aberrations were identified in 3 patients by CGH Analytics software. The horizontal and vertical axes indicate the position along 17p13.3 and the $\log_2$ ratio of the genomic copy number, respectively. The gray rectangles indicate regions of copy number aberrations. The dots indicate the annealing locations and the corresponding $\log_2$ ratios for each probe. The black dots indicate normal $\log_2$ ratio; whereas, red and green indicate $\log_2$ ratio higher than 0.5 and lower than −0.5, respectively. The red and black rectangles indicate locations of the previously reported CNVs and the known genes in the indicated regions. The names of the known genes are indicated below the figure, and *YWHAE*, *CRK*, and *LIS1* are highlighted in bold. (For interpretation of the references to color in this figure caption, the reader is referred to the web version of the article.)

In patient 2, a gain of genomic copy number was identified by aCGH in the MDS region containing *LIS1* (Fig. 1). The mean $\log_2$ signal ratios were +0.5 in chr17 (1,899,328–2,151,328) and +1 in chr17 (2,165,727–3,065,623), indicating duplication and triplication, respectively. These aberrations were confirmed by FISH analysis (Fig. 2B and Table 1), and fiber-FISH analyses revealed the directions of all triplicated segments with tandem insertions (Fig. 2D). The fact that neither parent of patient 2 showed any signal abnormalities in FISH analysis (data not shown) confirmed the de novo triplication in patient 2.

In patient 3, aCGH analysis revealed a terminal deletion of 17p, chr17 (1–1,280,058), which included *YWHAE* and *CRK*, but not *LIS1* (Fig. 1). This was confirmed by FISH analysis (Fig. 2C). The parental samples showed no abnormalities in this region (data not shown), indicating de novo deletion of 17p in patient 3.

Clinical reports

Patient 1 is a 22-year-old female was born at 38 gestational weeks with a weight of 2540 g (<25th centile). Since the patient showed no eye following and no responsive smiles at the age of 5 months, she was admitted to the hospital, and global agyria was identified by brain computed tomography (CT). In infancy, she started to suffer from several types of seizures, most of which were generalized tonic–clonic seizures, and an electroencephalography (EEG) examination showed irregular high-voltage slow waves with continuous multi-focal sharp waves (data not shown). These epileptic seizures were refractory to medical treatment. At the age of 16 years and 7 months, brain magnetic resonance imaging (MRI) analysis revealed lissencephaly with a predominance in the posterior region indicating grade 3 lissencephaly (Fig. 3A–C) (Kato and Dobyns, 2003). She

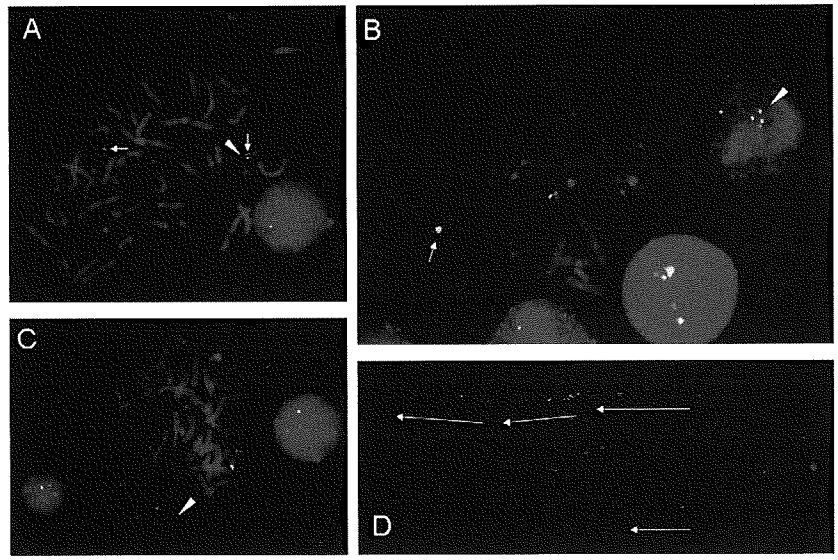

Figure 2 FISH and fiber-FISH analysis of the 3 patients. (A) Patient 1: partial deletion of *LIS1* was identified. The arrows indicate markers of chromosome 17 (RP11-1D5; red), and the arrowhead indicates the originally constructed partial sequence of *LIS1* (green). (B) Patient 2: duplication of *LIS1* was identified. FISH analysis indicated a predominant *LIS1* signal (RP11-135N5; green) in one allele of chromosome 17 (arrow) and increased *LIS1* signal numbers in metaphase (arrowhead). The red signals indicate markers, RP11-1D5. (C) Patient 3: one allele of *YWHAE* (RP11-356I18; green) is deleted (arrowhead). The red signals indicate markers, RP11-153A23. (D) Patient 2: fiber-FISH analysis identified a tandem triplication of the *LIS1* region in one of the chromosomal fibers. The green signals represent RP11-135N5, and the red signals represent CTD-2576K4. The arrows reflect a single unit of *LIS1* staining. The single arrow at the bottom represents a normal chromosome 17. (For interpretation of the references to color in this figure caption, the reader is referred to the web version of the article.)

was diagnosed with isolated lissencephaly because of her normal facial features (Fig. 4A). At 22 years of age, she showed good eye contact, visual tracking, social smiling, and various other facial expressions in response to parental vocalization, although she could not speak and had no head control. Epileptic seizures occurred several times a week. She was capable of taking oral paste foods and did not need tube feeding at home. Conventional G-banding chromosomal analysis showed a normal female karyotype (46,XX), and subsequent FISH analysis using a commercially available

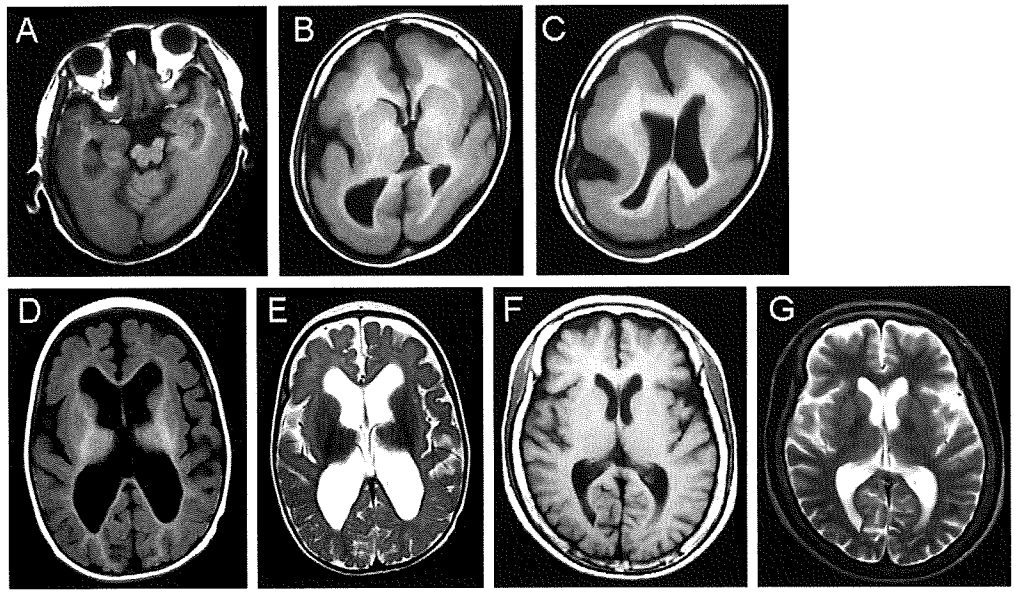

Figure 3 Brain MRI images of the three patients. (A–C) Grade 3 lissencephaly with predominant agyria in the posterior region was seen in patient 1. (D and E) Generalized hypoplasia of the brain involving the cortical and white matter regions was noted in patient 2. (F and G) Mild volume loss of the brain was identified in patient 3. (A–D, F) T1-weighted MRI image. (E and G) T2-weighted MRI image.

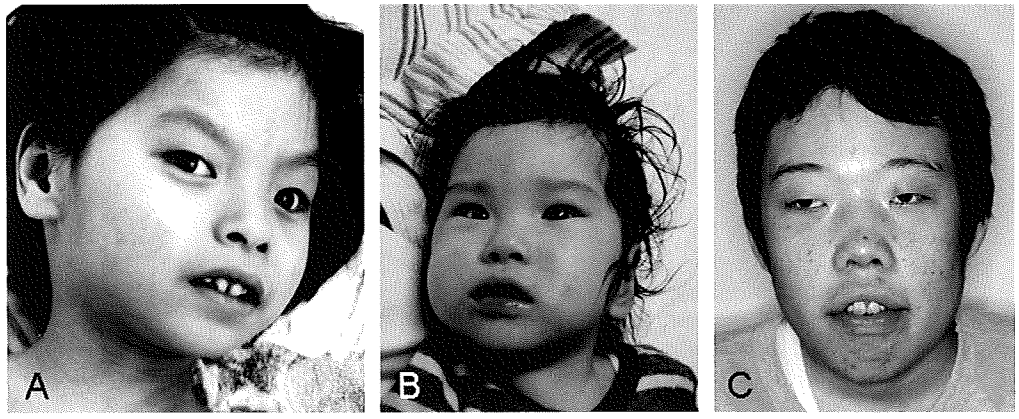

Figure 4 Portraits of the three patients. There were no distinct facial morphologies for patient 1 (A) or patient 2 (B). (C) Patient 3 showed a prominent forehead, bilateral ptosis, a broad nasal root, epicanthal folds, and retrognathia. Signed consent forms authorizing publication of the unmasked images of all identifiable patients have been obtained from the patients and/or their guardians.

probe, the Vysis Miller-Dieker Region/Isolated Lissencephaly Probe LSI *LIS1* (Abbott Laboratories, Abbott Park, IL, USA), indicated no deletion at 17p13.3 (data not shown).

Patient 2 is an 11-month-old girl was referred to us for infantile spasms. She was born at 39 weeks gestation with a birth weight of 1992 g (<3rd centile). At 6 months, her first epileptic seizure with deviation of eye position was noted, and EEG analysis showed modified hypsarrhythmia with synchronized high-voltage slow waves indicating West syndrome (Fig. 5). A subsequent brain MRI examination revealed generalized hypoplasia of the brain involving the cortical and white matter regions, associated with hypoplasia of the corpus callosum, which resulted in ventricular dilatation (Fig. 3C). Although several orally administered anti-epileptic drugs were ineffective, subsequent adrenocorticotropic hormone (ACTH) therapy was effective. At 6 months, she lacked neck control and could not roll over due to severe hypotonia. Conventional G-banding showed a normal female karyotype. At the age of 21 months, patient 2 showed an average growth rate with her length of 83.5 cm (=50th centile), weight of 10.0 kg (=50th centile), and head circumference of 47.0 cm (=50th centile). At this time, she was able to turn over but could not sit alone, indicating a severe developmental delay.

Patient 3 is a 23-year-old male was born to healthy parents at 39 weeks gestation with a birth weight of 2500 g (<50th centile). Delivery was uneventful. He suffered from mild developmental delay in infancy and from secondary generalized partial seizures at the age of 6 years. Subsequently, he suffered various types of seizures that were refractory to many different anti-epileptic drugs. Communication was challenging for him. At the age of 20 years, the Wechsler Adult Intelligence Scale (WAIS) indicated that his full IQ was 45 (verbal = 59, performance = 45). At the time of the study, he was working at a social welfare institution. His height was 155.5 cm (<3rd centile), his weight was 52.3 kg (<25th centile), and his head circumference was 56.2 cm (<25th centile). He had distinctive facial features (Fig. 4C). Conventional G-banding showed a normal male karyotype of 46,XY. A brain MRI examination revealed mild volume loss of the brain (Fig. 3F and G).

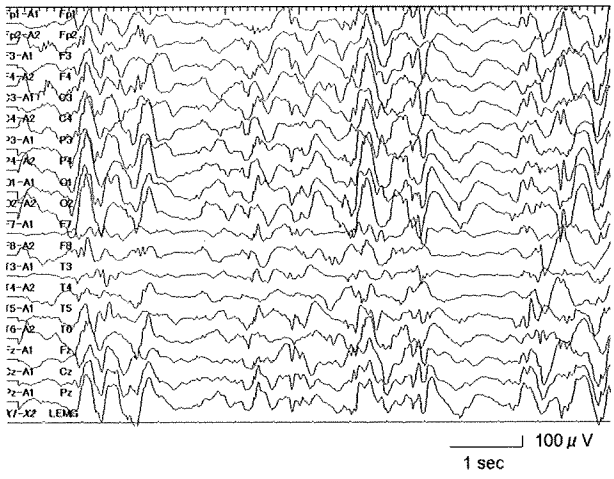

Figure 5 EEG analysis of patient 2, indicating modified hypsarrhythmia.

Discussion

In this study, we identified pathogenic CNVs in 17p13.3, the MDS critical region, in 3 epileptic patients.

Patient 1 had isolated grade 3 lissencephaly (Kato and Dobyns, 2003) but lacked the dysmorphic features common among MDS patients. As a commercially available *LIS1* probe did not detect deletion, aCGH analysis was performed and identified a microdeletion involving the last 5 exons of *LIS1*. This was similar to the findings of the previous report, in which FISH analysis using a commercially available *LIS1* probe yielded a false-negative result for a patient with a deletion in the 5′ region of *LIS1* (Izumi et al., 2007). In both cases, the incorrect analysis resulted from a partial *LIS1* deletion and from the limited availability of commercial FISH analysis probes. The deletion region of patient 1 included two other neighboring genes; *KIAA0664*, which encodes a hypothetical protein, and *GARNL4*, which encodes a GTPase-activating protein that activates the small guanine-nucleotide-binding protein Rap1 in platelets. Thus,